

Supplementary Materials: Molecular mechanisms associated with clustered lesion-induced impairment of 8-oxoG recognition by the human glycosylase OGG1

Tao Jiang², Antonio Monari^{1,3}, Elise Dumont^{2,4} and Emmanuelle Bignon^{1,*}

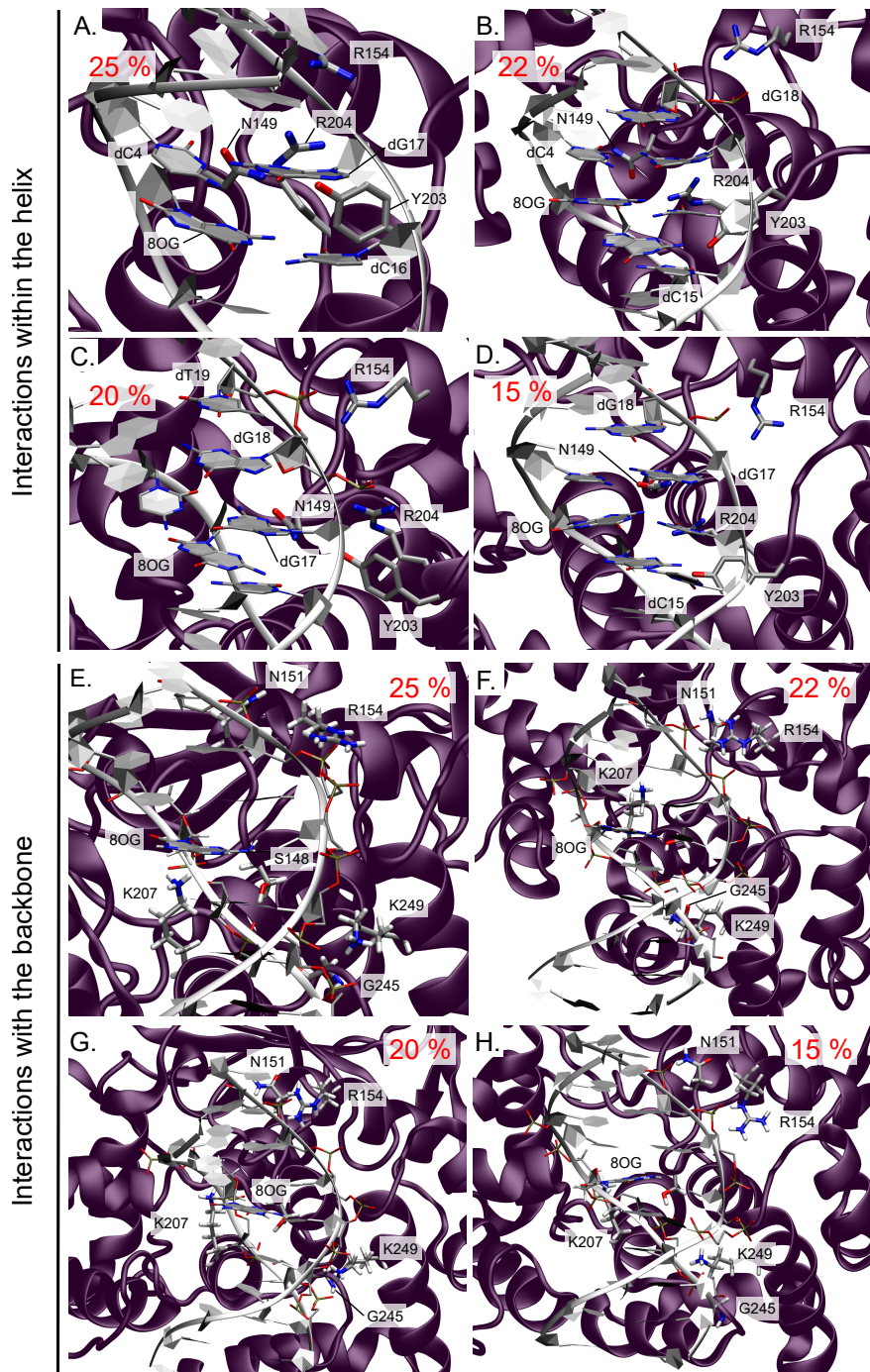


Figure S1. Representation of the key-interactions within the DNA helix (A. to D.) and with the DNA backbone (E. to H.) upon the presence of an isolated 8-oxoG for the four main clusters. The weight of the cluster is displayed in red.

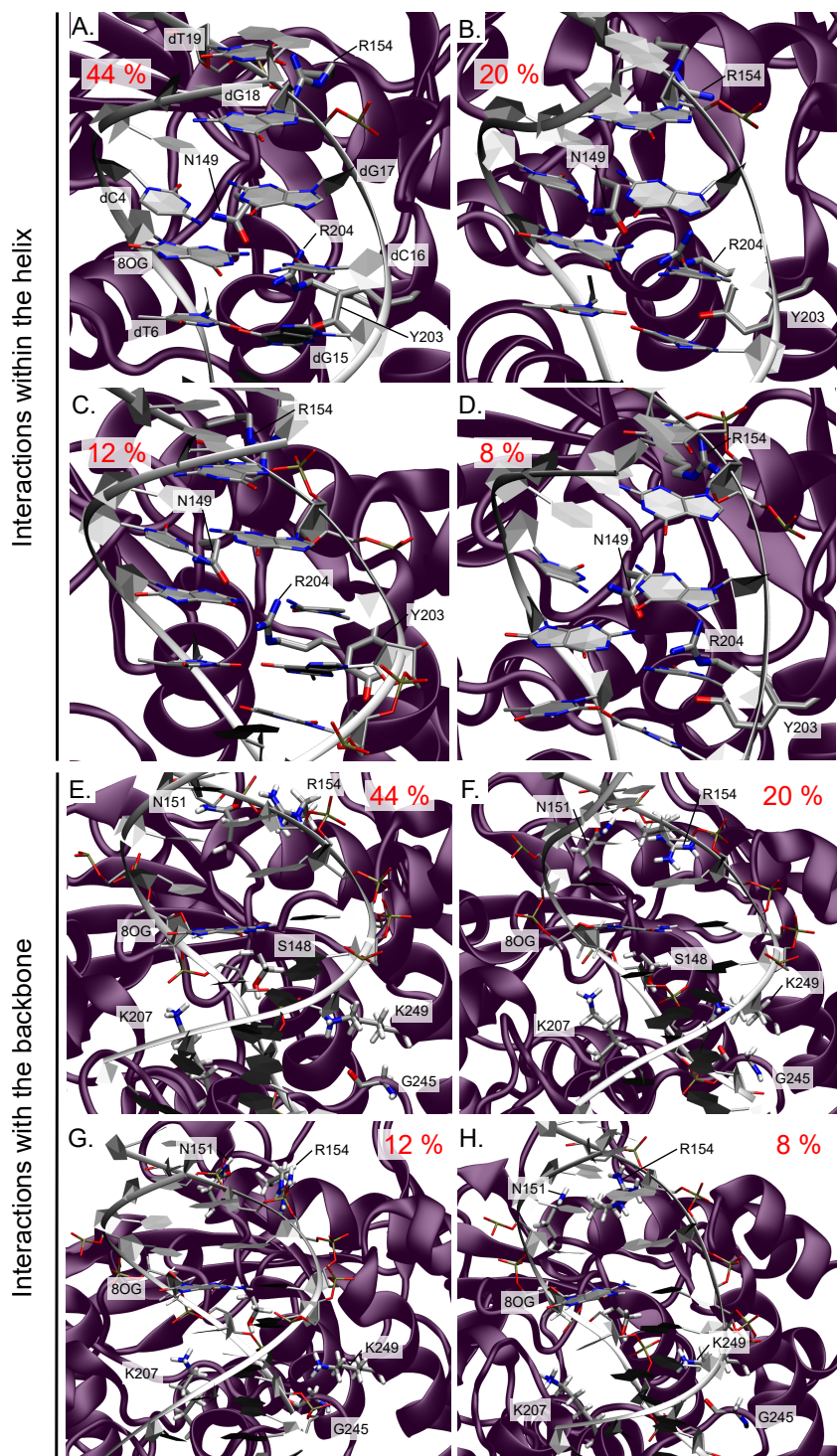


Figure S2. Representation of the key-interactions within the DNA helix (A. to D.) and with the DNA backbone (E. to H.) upon the presence of clustered 8-oxoG and 3' mismatch for the four main clusters. The weight of the cluster is displayed in red.

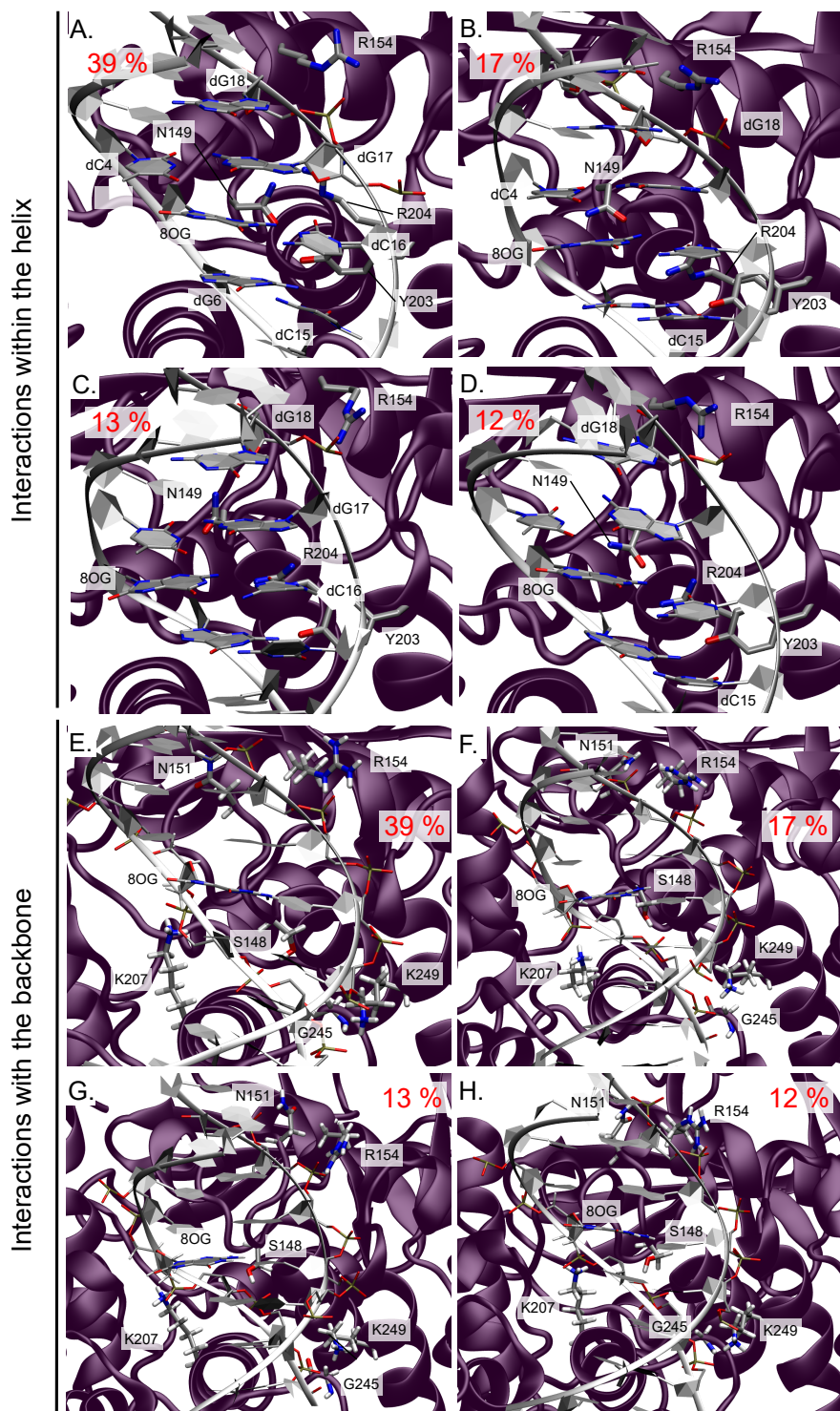


Figure S3. Representation of the key-interactions within the DNA helix (A. to D.) and with the DNA backbone (E. to H.) upon the presence of clustered 8-oxoG and 5' mismatch for the four main clusters. The weight of the cluster is displayed in red.

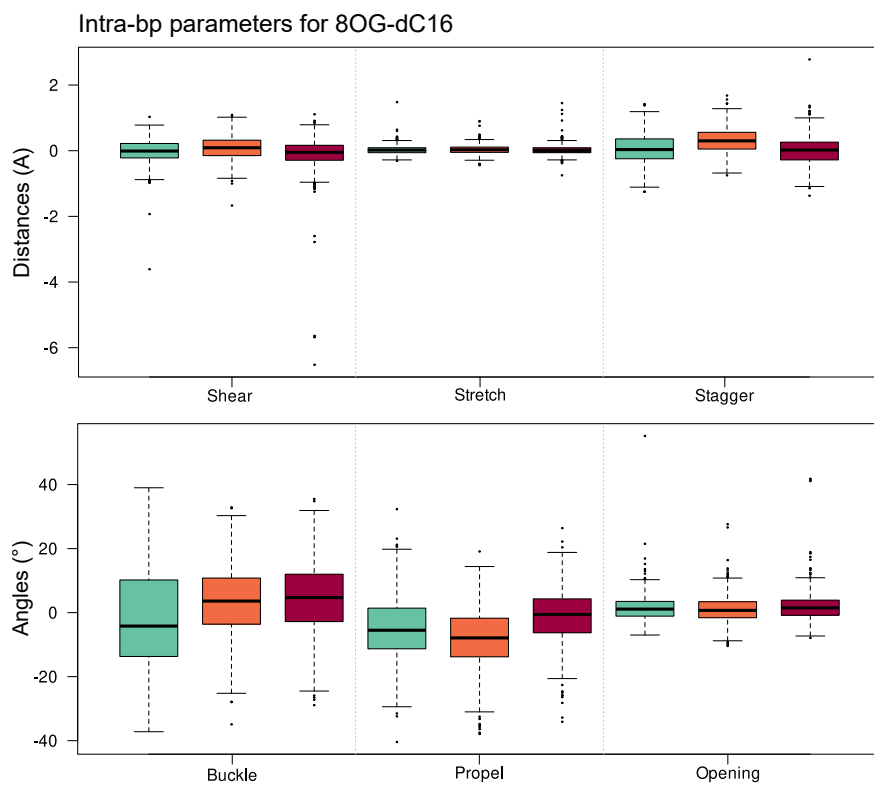


Figure S4. Intra-base pair structural parameters of the 8-oxoG-dC16 base pair in systems harboring an isolated 8-oxoG (cyan), clustered 8-oxoG + 3' mismatch (orange) or clustered 8-oxoG + 5' mismatch (red).

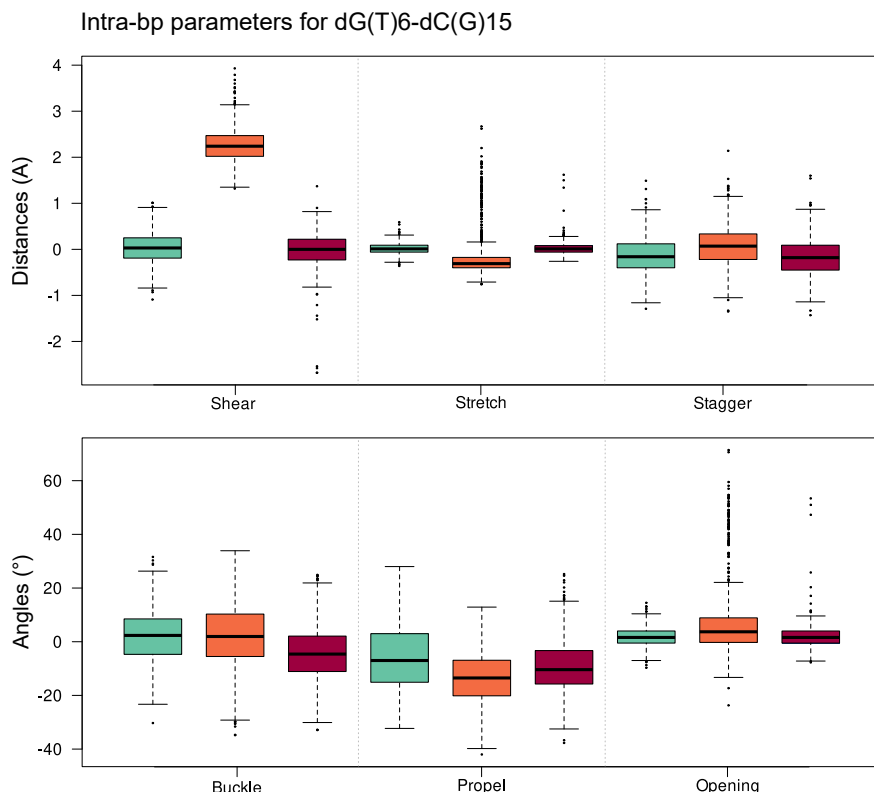


Figure S5. Intra-base pair structural parameters of the dG(T)6-dC(G)15 base pair 3' to the 8-oxoG in systems harboring an isolated 8-oxoG (cyan), clustered 8-oxoG + 3' mismatch (orange) or clustered 8-oxoG + 5' mismatch (red).

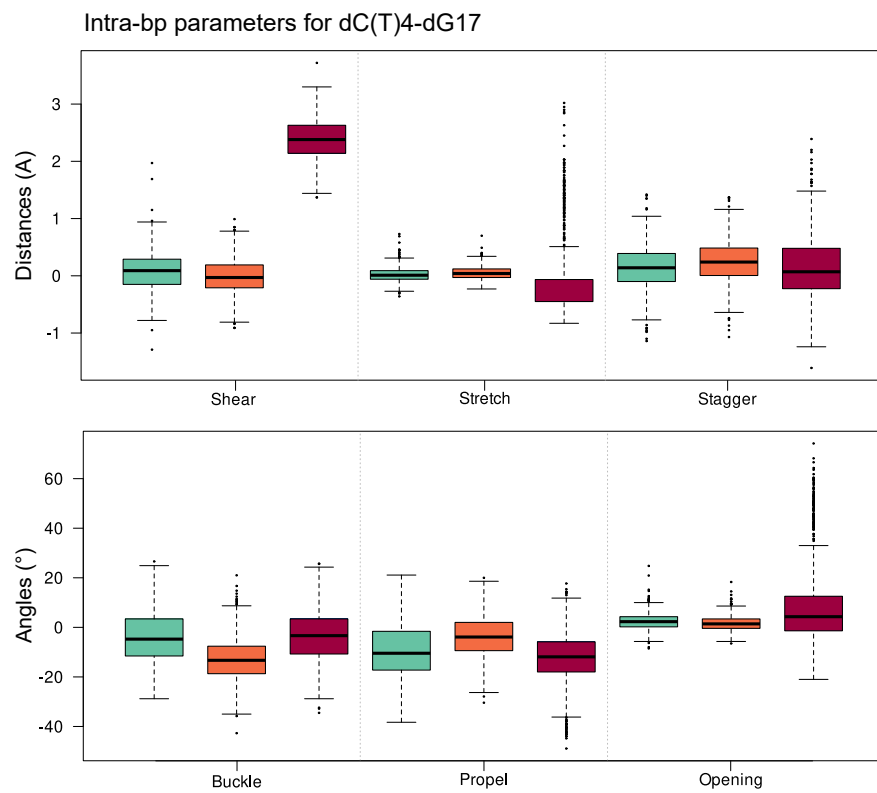


Figure S6. Intra-base pair structural parameters of the dC(T)4-dG17 base pair 3' to the 8-oxoG in systems harboring an isolated 8-oxoG (cyan), clustered 8-oxoG + 3' mismatch (orange) or clustered 8-oxoG + 5' mismatch (red).

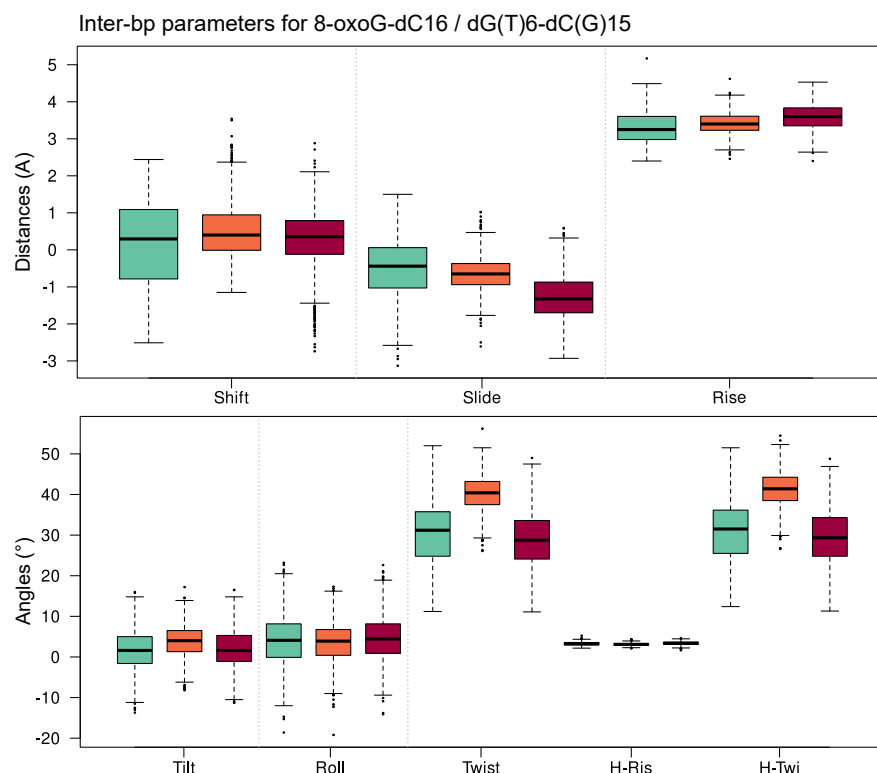


Figure S7. Inter-base pairs structural parameters of the 8-oxoG-dC16 / dG(T)6-dC(G)15 base pairs in systems harboring an isolated 8-oxoG (cyan), clustered 8-oxoG + 3' mismatch (orange) or clustered 8-oxoG + 5' mismatch (red).

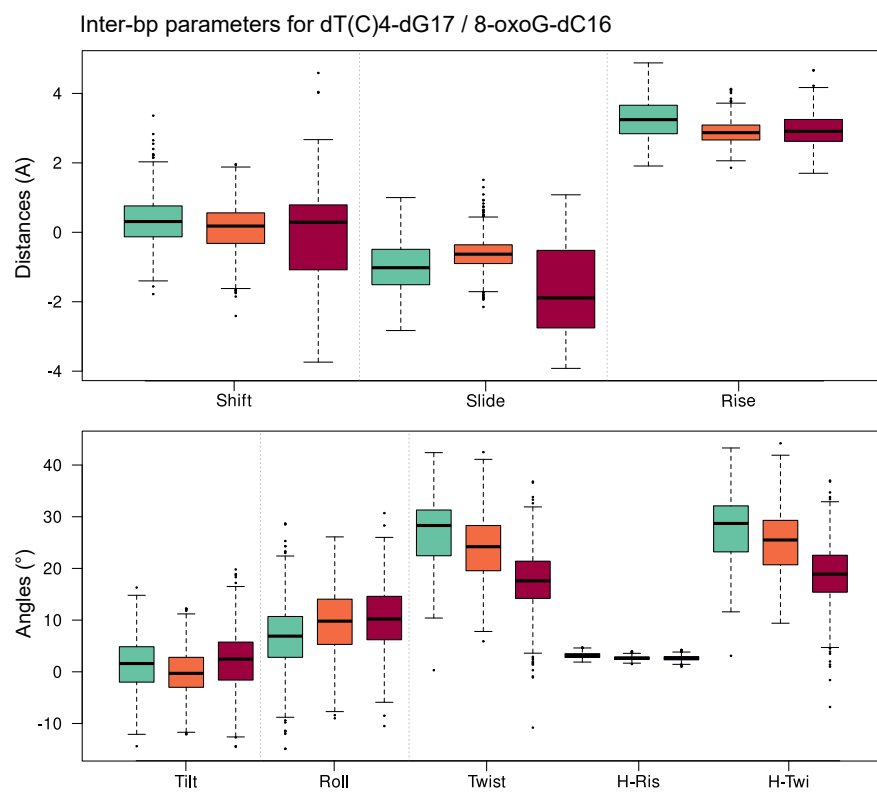


Figure S8. Inter-base pairs structural parameters of the dC(T)4-dG17 / 8-oxoG-dC16 base pairs in systems harboring an isolated 8-oxoG (cyan), clustered 8-oxoG + 3' mismatch (orange) or clustered 8-oxoG + 5' mismatch (red).

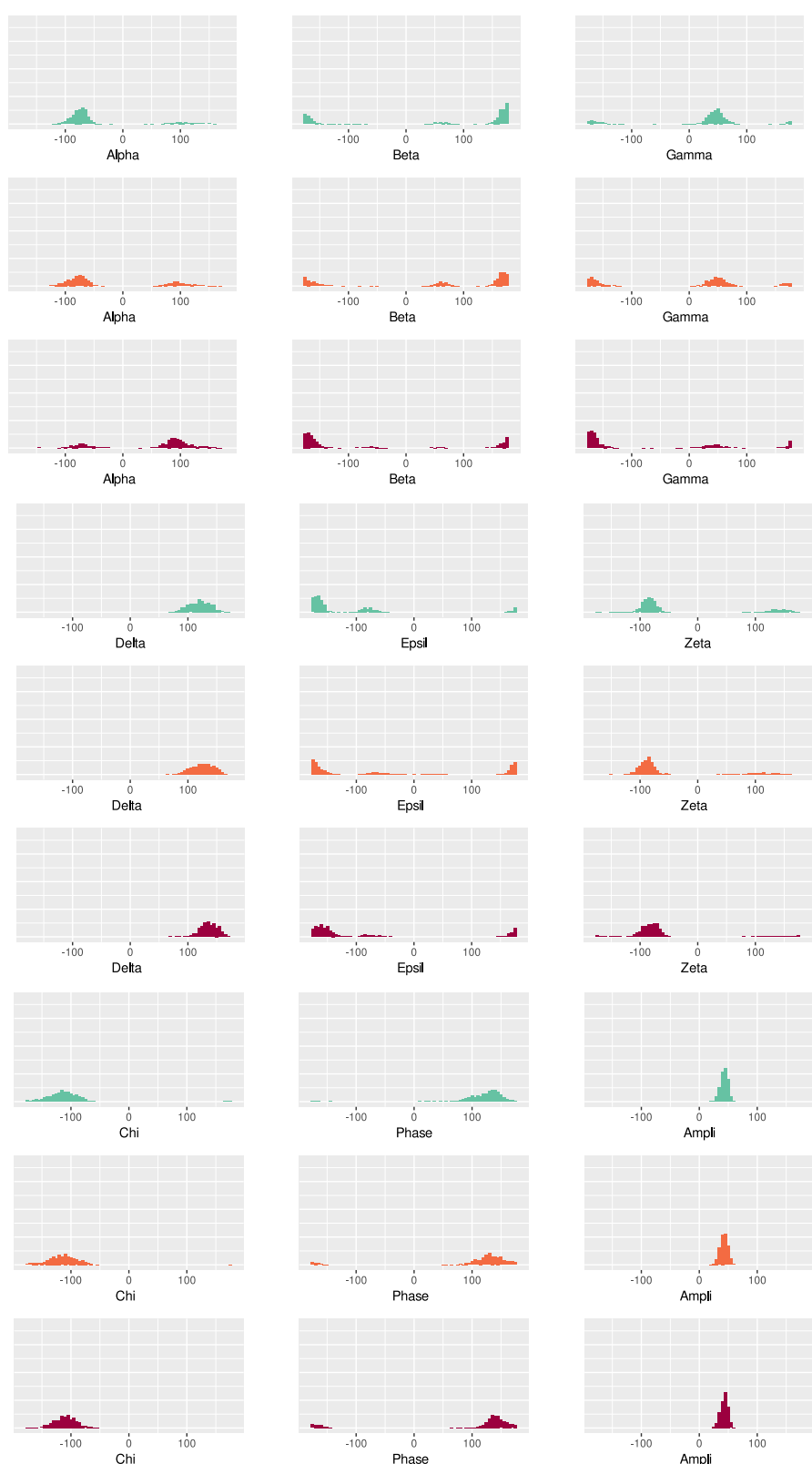


Figure S9. Distribution of 8-oxoG backbone angles values in systems harboring an isolated 8-oxoG (cyan), clustered 8-oxoG + 3' mismatch (orange) or clustered 8-oxoG + 5' mismatch (red).

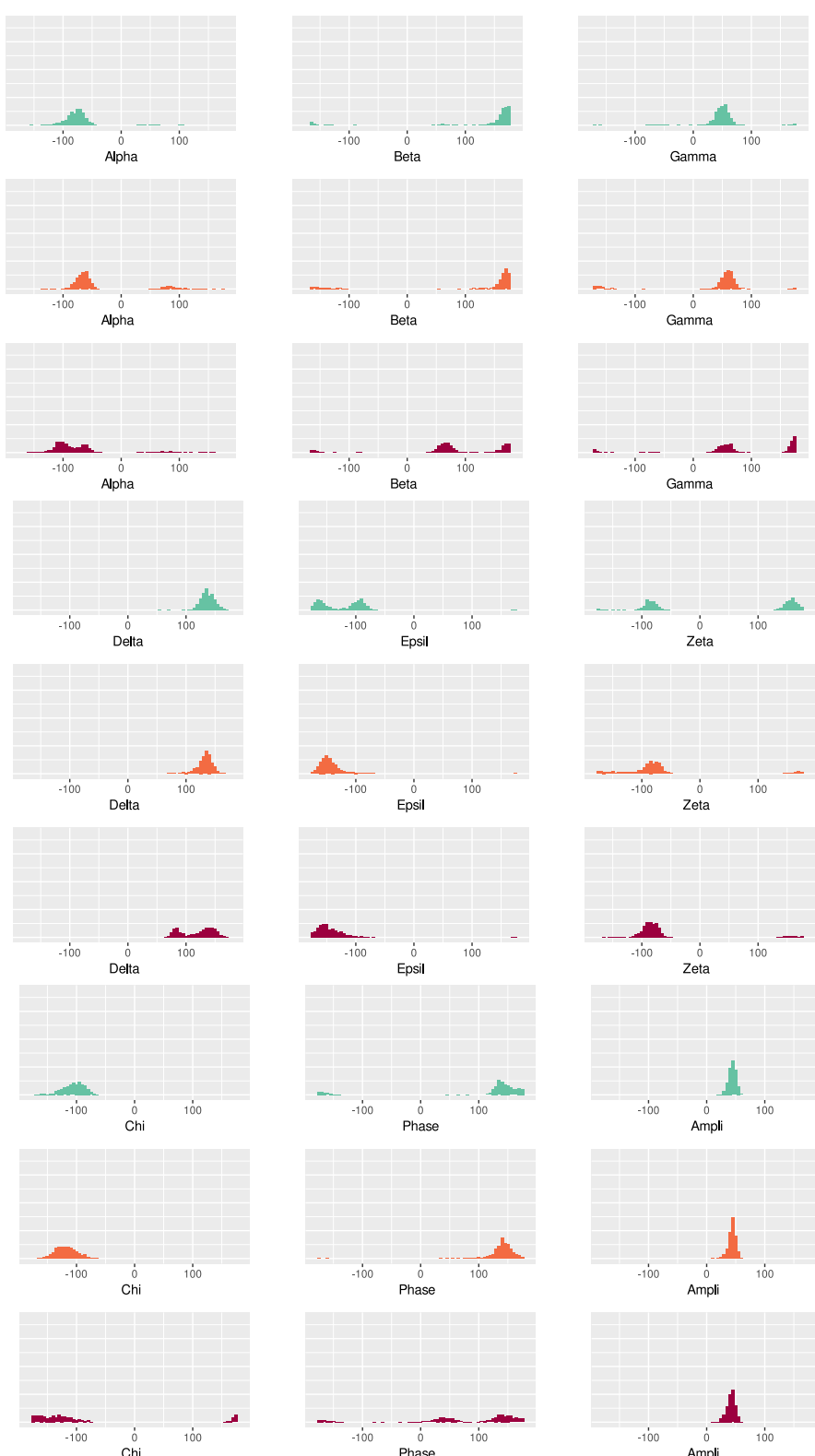


Figure S10. Distribution of dG(T)6 backbone angles values in systems harboring an isolated 8-oxoG (cyan), clustered 8-oxoG + 3' mismatch (orange) or clustered 8-oxoG + 5' mismatch (red).

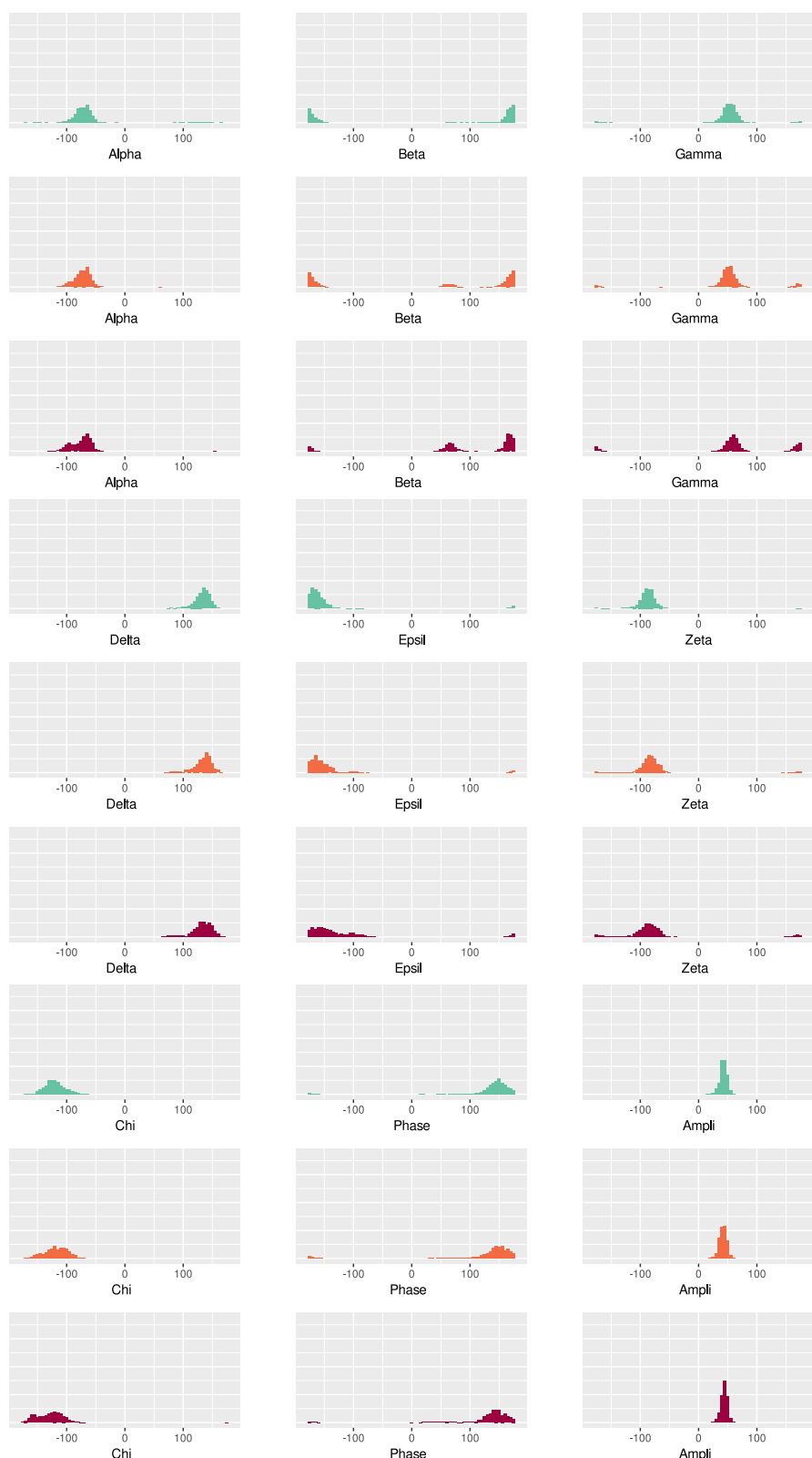


Figure S11. Distribution of the dC(T)4 backbone angles values in systems harboring an isolated 8-oxoG (cyan), clustered 8-oxoG + 3' mismatch (orange) or clustered 8-oxoG + 5' mismatch (red).

